J Solid State Electrochem (2012) 16:3237–3244
DOI 10.1007/s10008-012-1734-3

ORIGINAL PAPER

# Electrochemical behavior of nickel in electrolytes based on 1-*n*-butyl-3-methylimidazolium tetrafluoroborate ionic liquid for capacitor applications

**Fernanda Trombetta da Silva · Natália Fanti Panno · Michèle Oberson de Souza · Roberto Fernando de Souza · Emilse Maria Agostini Martini**

Received: 6 November 2011 / Revised: 14 March 2012 / Accepted: 19 March 2012 / Published online: 13 May 2012
© Springer-Verlag 2012

**Abstract** Electrochemical studies were performed using Ni electrodes in solutions of a mixture of ethylene glycol or of γ-butyrolactone with 1-*n*-butyl-3-methylimidazolium tetrafluoroborate ionic liquid. The aim of the study was to evaluate the use of these systems in electrochemical double-layer capacitor. Cyclic voltammetry experiments showed a potential range at which the Ni electrode behaved as a polarizable electrode. Ni oxidizes at high anodic potentials. Inside the potential range without electrochemical activity, the capacitance and the solution resistance, which were evaluated by impedance electrochemical spectroscopy, were compared for the two solutions tested. Conductivity measurements of the electrolytes with different compositions were also acquired. The results of cyclic voltammetry indicated that the Ni has a wide electrochemical window and low current peak densities of oxidation in the γ-butyrolactone medium than in ethylene glycol medium. The γ-butyrolactone and 1-*n*-butyl-3-methylimidazolium tetrafluoroborate ionic liquid solutions had the highest conductivity values. Decreased 1-*n*-butyl-3-methylimidazolium tetrafluoroborate ionic liquid content in different solvent mixtures resulted in an increase in the capacitance value at the Ni/electrolyte interface. The highest capacitance values were obtained for Ni in ethylene glycol and 1-*n*-butyl-3-methylimidazolium tetrafluoroborate medium.

**Keywords** Electrochemical capacitors · Ionic liquids · Electrochemical impedance · Nickel · Ethylene glycol · γ-Butyrolactone

## Introduction

Capacitors are devices that store electric energy when subjected to an applied potential. Interest in the development of electrode and electrolyte materials for the manufacture of supercapacitors has been increasing in recent years, mainly due to the possibility to store large amounts of energy.

Capacitors may be classified as electrolytic or electrochemical [1]. Electrolytic capacitors are composed of two conductor electrodes separated by a dielectric. The capacitances vary between 0.1 and 1 μF/cm$^2$, which are typical values for non-conducting or semiconductor oxides [2]. Electrolytic capacitors present high capacitance per unit of volume but are unstable and the capacitance gradually decreases, especially if subjected to heat or high tension [3].

Electrochemical capacitors, also named supercapacitors or ultracapacitors, do not have a dielectric separating the electrodes and are a new option for energy storage. Double electrical layer capacitors are among several kinds of electrochemical capacitors [3, 4]. The capacitance results from the charge separation at the electrode/electrolyte interface. The capacitance for a double electrical layer capacitor varies between 10 and 100 μF/cm$^2$, which is much greater than the capacitance of an electrolytic capacitor [3].

**Electronic supplementary material** The online version of this article (doi:10.1007/s10008-012-1734-3) contains supplementary material, which is available to authorized users.

F. T. da Silva (✉) · N. F. Panno · M. O. de Souza · R. F. de Souza · E. M. A. Martini (✉)
Institute of Chemistry, UFRGS,
Av. Bento Gonçalves, 9500, P.O. Box 15003,
Porto Alegre 91501-970, Brazil
e-mail: fetrombetta@iq.ufrgs.br
e-mail: emilse@iq.ufrgs.br

When constructing a double-layer capacitor, the electrode material must be stable inside the electrolytic solution; therefore, Faradaic processes such as oxidation, corrosion, and oxide film formation are not desirable. For these reasons, there are many investigations searching for electrode materials that are not susceptible to corrosion, such as activated carbon [5–11], which is potentially useful for applications in electrochemical capacitors due to low cost, high-specific area, and high stability. A greater specific surface area of carbon leads to a greater specific capacitance. However, only part of the carbon surface area is electrochemically accessible when in contact with the electrolyte in other words, the gravimetric capacity of several carbon materials does not increase linearly with the surface area. This behavior constitutes a technical problem because it can cause a failure in the capacitor specification.

This work tests Ni as the electrode material of an electrochemical capacitor. The use of Ni was suggested for the construction of pseudocapacitive-type electrochemical capacitors, where the pseudocapacitance arises from reversible Faradaic redox reactions. Previous reports indicate that Ni and Ni oxide or hydroxide show high electrochemical activity in alkali electrolytes, which is the origin of pseudocapacitance [12–15]. Ni is a component of several steel alloys because it is resistant to air and water corrosion. Ni is also corrosion resistant in other aggressive media and is stable at high temperatures. Due to these properties, Ni is used as an electrically deposited protective coating because it is metallurgically compatible with a great variety of elements. Ni electrodes are important materials for electrochemical applications and in devices for energy conversion. In aqueous solutions, a $Ni(OH)_2$ film is initially formed on a Ni surface and gradually converted to NiO or NiOOH, which is dependent on the pH and potential applied [16–18].

The capacitors are impregnated with electrolytic solutions constituted by aqueous or non-aqueous solvents and dissolved salts that improve conductivity as well as corrosion inhibitors, dielectric oxide stabilizers, and gas absorbers. The choice of an adequate electrolyte is very important because it is responsible for the capacitor performance because charge separation occurs at the dielectric/solution interface (electrolytic capacitors) or at the electrode/solution interface (electrochemical capacitors) [1]. Aqueous electrolytes are best to ensure the solubility of salts and the required conductivity is achieved due to a high relative permittivity.

The low decomposition potentials by water electrolysis, the high vapor pressure, and the possibility of dielectric or metallic surface damage causes the use of high amounts of water in the electrolytic mixture to be undesirable [19]. A possible solution to this problem is the use of polar organic solvents that have high relative permittivity, such as ethylene glycol (EG) and γ-butyrolactone (GBL), in the composition of capacitor impregnation electrolytes [1]. A limitation for using these solvents is their low conductivity, which often does not meet the specifications required for the production of small capacitors with low impedance. Therefore, researchers continue to investigate new electrolytic systems, which are non-aqueous but consist of ionic electrolytes. High thermal stability and high boiling temperatures are extremely necessary for application in small capacitor.

Ionic liquids are molten salts at room temperature and can be synthesized with a great diversity of cations and anions, which are used as electrolytes in several electrochemical applications, such as solvents for electrodeposition, batteries, fuel cells, and others [20–25]. Ionic liquids present many attractive properties, such as thermal stability, inflammability, high ionic conductivity, a large electrochemical window, and negligible vapor pressure, and they are not corrosive [26–36]. Ionic liquids are also considered to be "green solvents" because they are nontoxic [30]. The properties of ionic liquids meet the property requirements for the electrolyte component of capacitors.

This study investigates the electrochemical behavior of Ni in electrolytic mixtures consisting of EG or GBL with 1-*n*-butyl-3-methylimidazolium tetrafluoroborate ionic liquid, with the target application being the production of electrochemical capacitors. The techniques used in this study were potentiodynamic polarization, electrochemical impedance spectroscopy, and conductivity measurements.

## Experimental

Initially, the 1-*n*-butyl-3-methylimidazolium tetrafluoroborate ionic liquid ($BMI.BF_4$) was prepared according to previously published procedures [37, 38]. The ionic liquid was synthesized under an argon atmosphere and dried under reduced pressure. The water content (200 ppm) was determined using a coulometric Karl Fischer titration (Titrino 756 KF Metrohm). The proton nuclear magnetic resonance analysis was performed in order to verify the purity of the $BMI.BF_4$ using a spectrometer Varian VXR 300 (300 MHz) in $CDCl_3$ and at room temperature.

The electrolytic solutions were prepared in a total volume of 5.0 mL using different mixtures of EG (Merck) or GBL (Reagen-Quimibrás) with $BMI.BF_4$. Volumetric percentages of 100 % $BMI.BF_4$, 80 % $BMI.BF_4$, 60 % $BMI.BF_4$, 40 % $BMI.BF_4$, and 20 % $BMI.BF_4$ were used. Table 1 presents the molar concentration of $BMI.BF_4$/EG and $BMI.BF_4$/GBL mixtures as a function of the volumetric percentage.

The electrochemical experiments were performed using a conventional three-electrode analytical cell with a platinum network counter electrode and a platinum wire quasi-reference electrode (QSR-Pt). As the solutions are not aqueous, the use of a traditional reference electrode is not recommended because of the formation of a liquid junction which can cause a

**Table 1** Molar concentration and open circuit potential (OCP) of $BMI.BF_4$/EG and $BMI.BF_4$/GBL mixtures

| % (*v*/v) $BMI.BF_4$ | $C_{EG}$ (mol/L) | $C_{GBL}$ (mol/L) | $C_{BMI.BF4}$ (mol/L) | $E_{OCP}$ (*V*) (QSR-Pt) EG | $E_{OCP}$ (*V*) (QSR-Pt) GBL |
|---|---|---|---|---|---|
| 100 | 0.00 | 0.00 | 5.35 | −0.223 | −0.223 |
| 80 | 3.58 | 2.62 | 4.28 | −0.130 | −0.262 |
| 60 | 7.15 | 5.25 | 3.71 | −0.291 | −0.297 |
| 40 | 10.7 | 7.87 | 2.14 | −0.320 | −0.200 |
| 20 | 14.3 | 10.50 | 1.07 | −0.324 | −0.296 |

potential gradient to develop due to the diffusion of ions across the junction. When ionic liquids are used as the electrolyte in electrochemical experiments, a platinum or silver wire is usually employed as the reference electrode [39–41]. The working electrode consisted of a pure Ni disk (99.99 %, Goodfellow), which was inserted in a Teflon holder with an exposed area of 0.2 cm². The disk was polished with 400, 600, and 1,200 grit emery papers and washed with distilled water and ethanol prior to drying.

The electrochemical measurements were performed with an Autolab model PGSTAT 30 potentiostat coupled with a frequency response analyzer for impedance spectroscopy and with a GPES module for cyclic voltammetry. The experiments were performed at room temperature and under an argon atmosphere.

Electrochemical impedance spectroscopy analyses were performed at the open circuit potential (OCP) over a frequency range of 100 mHz to 100 kHz and at an amplitude of 10 mV. Impedance was measured after the electrodes were immersed in the solutions for 1 h. Cyclic voltammetric experiments were then performed. The electrode potential scan rate was set to 0.010 V/s, and the potential was scanned between the limits of −2.0 and +2.0 V (QSR-Pt). The first scan is reported. The conductivity ($\sigma$) of all solutions was measured at room temperature, using a Hach SensIon 7 conductivity meter.

## Results and discussion

Figure 1 (inset) presents the cyclic voltammogram of the Ni electrode in $BMI.BF_4$. The initial cathodic current of the potential scan may be related to a hydrogen evolution reaction due to the reduction of residual water or to the decomposition of the ionic liquid [39]. In the anodic potential range, one anodic peak at +1.55 V (QSR-Pt) attributed to the oxidation of the $Ni^0$ to Ni(II) species is observed in the voltammogram of Ni in $BMI.BF_4$. The potential of the oxidation peak is shifted to more positive values when compared to aqueous medium [11]. In non-aqueous solution with lower conductivity, the ohmic drop results in a lower electrodic potential than what is actually being applied. In the reverse scan, the cathodic peak at −1.53 V (QSR-Pt), which corresponded to Ni(II) reduction to $Ni^0$, shows the presence of a $Ni^0$/Ni(II) redox pair. There is a potential range between the peaks without Faradaic processes, in which Ni behaves as a polarizable electrode. In this potential range, the increased potential results in charge storage at the Ni/ionic liquid interface, which characterizes the system as having a capacitive behavior.

Electrochemical impedance spectroscopy was performed to characterize the capacitive behavior of the Ni/$BMI.BF_4$ interface at the OCP. The OCP was within the potential range at which the Ni electrode did not present charge-transfer Faradaic processes (see Table 1). Figure 2a and 2b are Nyquist and Bode diagrams, which were obtained from the impedance experiments. An evidence for capacitive behavior of the system was provided by inclined capacitive line. Further evidence was provided in the Bode diagram: the slope was nearly −1 in log $|Z|$ versus log $f$ in the low to intermediate frequency range, there was an absence of a resistance horizontal line at low frequencies and the phase angle was nearly 90°. The capacitance at the Ni/$BMI.BF_4$ interface was calculated by $C = 1/(2\pi f_{max} Z)$, where the $f_{max}$ is the frequency of the maximum value of phase angle in the Bode diagram (log $|Z|$ versus $\theta$) and the impedance $Z$ was

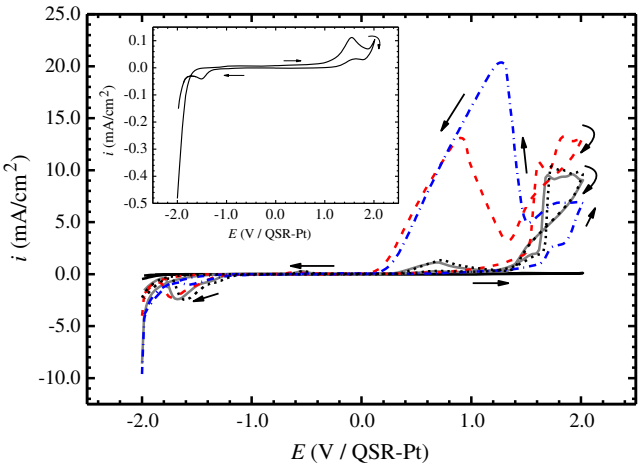


**Fig. 1** Cyclic voltammograms of Ni in $BMI.BF_4$/EG mixtures. The solvent systems are 20 % (*v*/*v*) $BMI.BF_4$ (*black broken line*), 40 % (*v*/*v*) $BMI.BF_4$ (*blue broken line*), 60 % (*v*/*v*) $BMI.BF_4$ (*red broken line*), 80 % (*v*/*v*) $BMI.BF_4$ (*gray solid line*) and 100 % (*v*) $BMI.BF_4$ (*black solid line*) with a magnified inset. The potential scan rate was 0.010 V/**s**

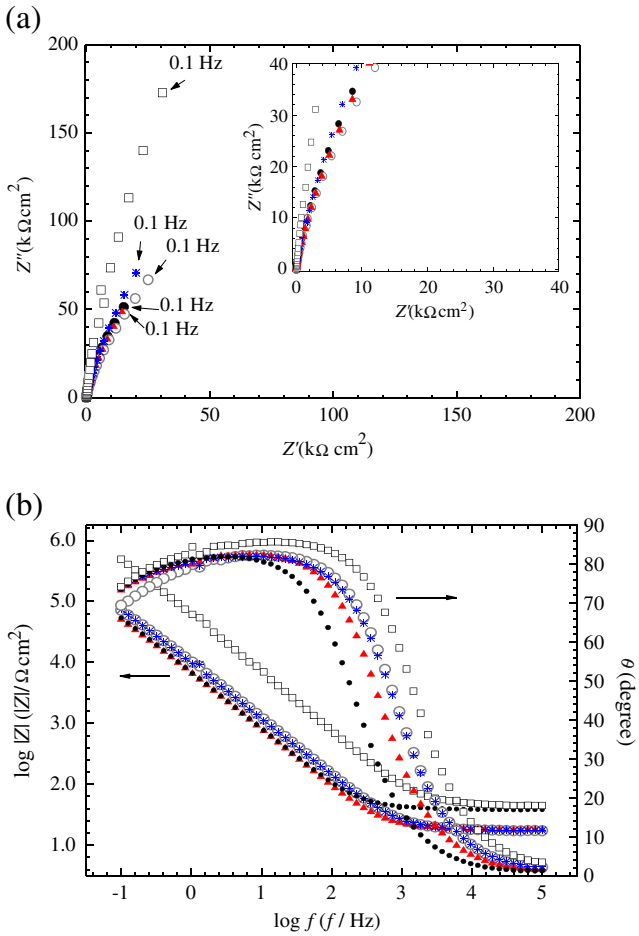


**Fig. 2** Nyquist (2a) and Bode (2b) impedance diagrams of Ni in $BMI.BF_4$/EG mixtures at OCP (QSR-Pt): 20 % (*v*/*v*) $BMI.BF_4$ (*filled circle*), 40 % (*v*/*v*) $BMI.BF_4$ (*asterisk*), 60 % (*v*/*v*) $BMI.BF_4$ (*filled triangle*), 80 % (*v*/*v*) $BMI.BF_4$ (*empty circle*), and 100 % (*v*) $BMI.BF_4$ (*empty square*)

obtained from this frequency (log $|Z|$ versus log $f$). The resistance in high frequency, associated with solution resistance ($R_S$), was calculated considering $\log Z_{f\to\infty} = \log R_s$, where the total impedance is constant in relation to the frequency. These treatments were applied to all impedance experiments.

### 1. *EG and BMI.BF$_4$ mixtures*

Figure 2a and 2b show the Nyquist and Bode diagrams, respectively, obtained for Ni at OCP in different solutions of $BMI.BF_4$ and EG. Although the addition of EG into $BMI.BF_4$ affects the capacitance properties, these solutions present an inclined capacitive line. The Bode diagram (log $|Z|$ versus log $f$) presents a capacitive straight line with a slope of −1 at low and intermediate frequencies and a horizontal line at high frequencies, which is associated with $R_S$. Both the diagrams and a phase angle near 90° at log $|Z|$ versus $\theta$ prove the capacitive behavior of the Ni/electrolyte interface, which is similar to its behavior in pure $BMI.BF_4$. Increasing the amount of EG results in a decrease in the total impedance of the system at the same frequency (Fig. 2b). The phase angle also decreases and the capacitive straight line shifts to lower frequency values. These results point to a decrease in the capacitive reactance of the Ni/electrolyte interface as the amount of EG in the mixture increase, which leads to an increase in the capacitance and the charge stored at the interface. The impedance associated with $R_S$ decreases as the amount of EG in the mixture increases until *ca*. 60 % (*v*/*v*) $BMI.BF_4$, which begins to increase upon further addition.

The cyclic voltammograms of Ni immersed in the $BMI.BF_4$/EG mixtures (Fig. 1) resulted in the observation of a potential range without electrochemical activity. The OCP values where the impedance experiments were performed were included in this range (see Table 1), which justifies the capacitive behavior of the impedance diagrams. During direct scan potential, the voltammograms showed an increase in the anodic current without the observation of characteristic $Ni^0$ to Ni (II) oxidation peak. Probably, this peak is concealed or covered by increased anodic current when the EG amount increases (see Electronic supplementary material).

With the potential inversion, an anodic reactivation peak appears. The reactivation peak causes high current densities in $BMI.BF_4$/EG mixtures with low $R_S$, i.e., with high conductivity. The current density of the anodic reactivation peak is larger than the current density obtained from the direct scan at the same potential values. The resulting hysteresis indicates that an increase of the dissolutive oxidation rate of Ni occurred, which is most likely due to the increase of the active electrodic area. This behavior can be attributed to the presence of an oxide film on the surface of the electrode, which formed during preparation and is removed as a potential is applied (direct scan). When the potential scan is reversed, the oxidation occurs at a high rate due to an increase in the amount of exposed metallic Ni. The conclusion is that the anodic polarization of Ni in $BMI.BF_4$/EG mixtures lead to the dissolution of the metallic surface. The use of EG as a solvent for the electrolyte [42–44] and as a co-solvent with a choline chloride based ionic liquid [45] have been previously described in electrochemical polishing procedures. The studies regarding the electropolishing process with EG and $BMI.BF_4$ mixtures showed that there is a formation of a viscous layer at the metal surface. The positive Faradaic current flows due to the dissolution of the metal oxide on the surface and the dissolution of metal through the oxide holes. The removal of the oxide is a relatively slow process. The oxide dissolution and metallic anodic oxidation are controlled by diffusion through the viscous layer. Any anodic oxide formation on the metallic surface that can interfere with the process is prevented.

## 2. *GBL and BMI.BF$_4$ mixtures*

The Nyquist and Bode diagrams obtained for Ni at OCP in different BMI.BF$_4$/GBL solutions are acquired after 1 h of immersion and are presented in Fig. 2a and 2b, respectively. Similar to the results for the BMI.BF$_4$/EG solutions, the spectra show an inclined capacitive line in the Nyquist diagram and a phase angle near 90° and straight line with a slope of −1 in the Bode diagram. These results indicate that capacitive behavior occurs at the Ni/electrolyte interface. Increased amounts of GBL lead to a decrease in the total impedance of the system (Fig. 3a, 3b).

The cyclic voltammograms for all solvent mixtures (Fig. 4) show a cathodic current at the beginning of the scan, which is associated with a hydrogen evolution reaction or with the decomposition of ionic liquid.

In the anodic scan, a peak appears near +0.25 V (QSR-Pt) in 20 % BMI.BF$_4$ (*v*/*v*), which shifts to +0.50 V (QSR-Pt) in 80 % BMI.BF$_4$ (*v*/*v*). A second anodic peak is present at +1.5 V (QSR-Pt), which is not significantly affected by the amount of GBL added to the mixture. This peak is not present in 40 % BMI.BF$_4$ (*v*/*v*) probably because it shifted to higher values, coinciding with potential reversion. These peaks can be attributed to the oxidation of different allotropes of $Ni^0$ to Ni(II) species. Near the reversal potential, the anodic current increases. At +2.0 V (QSR-Pt), as the scan is reversed, the anodic current is high for mixtures with low content of BMI.BF$_4$, which corresponds to solutions with low $R_S$. In the reverse scan, one cathodic peak, associated with the reduction of Ni (II) that was previously formed, is observed in the voltammagrams, which indicates that the electrochemical process is reversible. The cathodic current peak also increased and shifts to higher values of potential for mixtures with low content of BMI.BF$_4$, therefore with low $R_S$. The anodic and cathodic current peak densities are smaller than those observed in the system containing EG, which is most likely due to the greater stability of the Ni electrode relative to the charge transfer reactions in the GBL medium.

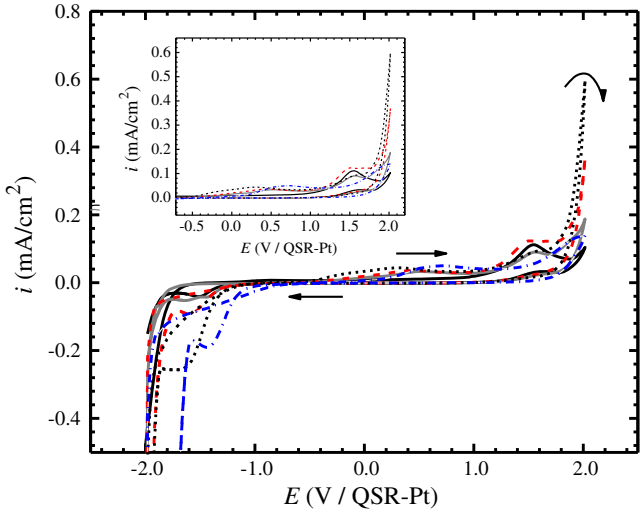


**Fig. 4** Cyclic voltammograms of Ni in BMI.BF$_4$/GBL mixtures. The solvent systems are 20 % (*v*/*v*) BMI.BF$_4$ (*black broken line*); 40 % (*v*/*v*) BMI.BF$_4$ (*blue broken line*), 60 % (*v*/*v*) BMI.BF$_4$ (*red broken line*), 80 % (*v*/*v*) BMI.BF$_4$ (*gray solid line*), and 100 % (*v*) BMI.BF$_4$ (*black solid line*). The potential scan rate was 0.010 V/s

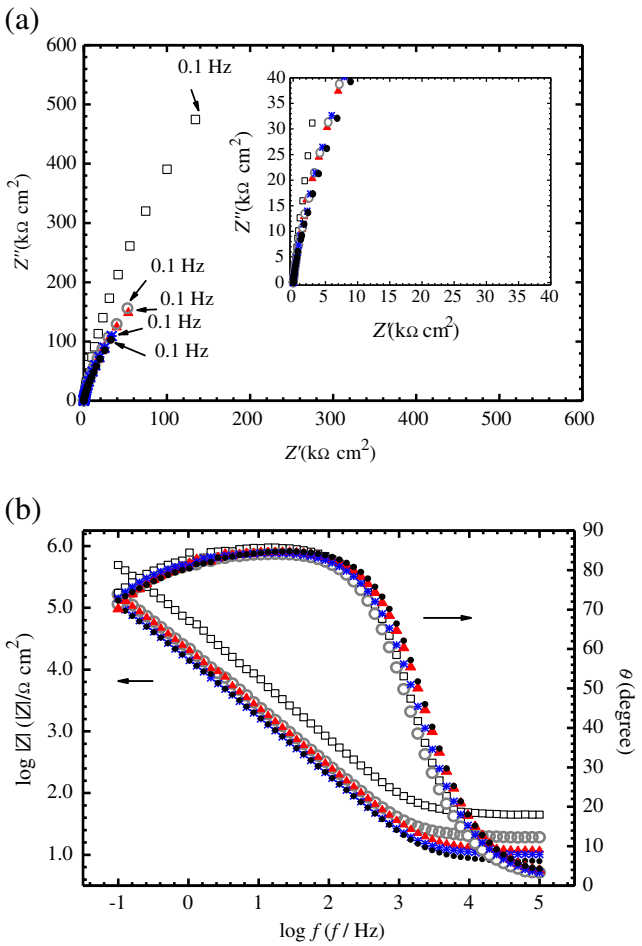


**Fig. 3** Nyquist (3a) and Bode (3b) impedance diagrams of Ni in BMI.BF$_4$/GBL mixtures at OCP (QSR-Pt): 20 % (*v*/*v*) BMI.BF$_4$ (*filled circle*), 40 % (*v*/*v*) BMI.BF$_4$ (*asterisk*), 60 % (*v*/*v*) BMI.BF$_4$ (*filled triangle*), 80 % (*v*/*v*) BMI.BF$_4$ (*empty circle*), and 100 % (*v*) BMI.BF$_4$ (*empty square*)

## 3. *EG* versus *GBL in mixtures containing BMI.BF$_4$*

The $R_S$ is obtained through a Bode plot (log $|Z|$ versus log $f$), where the total impedance is constant in relation to the frequency. For the application in electrochemical capacitors, particularly low impedance capacitors, the impregnation solutions are required to have a small series resistance, which is responsible for fast capacitor charging and discharging during cycles. The $R_S$ is an important factor for the operation of an electrochemical system because it promotes power dissipation. A reduction in $R_S$ caused by an increase in the conductivity of the impregnation solution

would cause the power dissipation to decrease, which would lead to solution heating.

Figure 5 shows the $R_S$ values obtained as a function of the mixture BMI.$BF_4$ and EG composition. These results indicate that increased BMI.$BF_4$ amounts cause a decrease in the solution resistance until a minimum value is reached and then increases again until 100 % BMI.$BF_4$. In pure BMI.$BF_4$, the cations $BMI^+$ and anions $BF_4^-$ are slightly dissociated and the solution conductivity is low because there are strong Coulomb interactions [46]. As EG was added, the dissociation processes of BMI.$BF_4$ was improved, due to the decrease of Coulomb interactions and the release of free ions from their associates and aggregates [47]. The increase in the conductivity of a given system must be due to the increase in ion mobility and/or the number of charge carriers. Consequently, the conductivity of the mixture increases, which decreases the $R_S$ values. In EG-rich solutions, the low BMI.$BF_4$ content causes an increase in solution resistance. Therefore, solutions containing 40, 60, and 80 % (*v*/*v*) of BMI.$BF_4$ in EG have the highest possibility to be used as electrolytes in the manufacture of electrochemical double-layer capacitors with Ni electrodes.

Figure 5 also presents the $R_S$ values obtained as a function of the BMI.$BF_4$/GBL mixture composition. The results show that $R_S$ increases exponentially as the BMI.$BF_4$ content increases, which indicates that by raising the GBL amount, the degree of dissociation is enhanced and the solution becomes more conductive [47].

The conductivities of BMI.$BF_4$ mixtures in EG or GBL at room temperature were also evaluated and are presented in Table 2. In the EG medium, the conductivity increases concomitantly with the BMI.$BF_4$ content until a maximum value (80 % BMI.$BF_4$) is reached, and then the conductivity decreases. In the GBL medium, the conductivity decreases

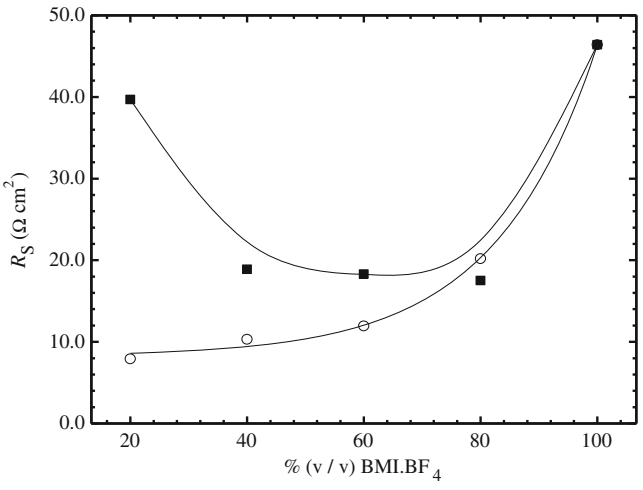


**Fig. 5** A plot of the solution resistance ($R_S$) for the Ni electrode as a function of the volumetric percentage of BMI.$BF_4$ in EG (*filled square*) or GBL (*empty circle*) and BMI.$BF_4$ mixtures

**Table 2** Conductivity BMI.$BF_4$/EG and BMI.$BF_4$/GBL mixtures at 30 °C

| | % (*v*/*v*) BMI.$BF_4$ | 20 | 50 | 80 | 100 |
|---|---|---|---|---|---|
| $\sigma$ (mS/cm) | EG | 4.8 | 9.7 | 11.8 | 5.2 |
| | GBL | 19.4 | 16.4 | 12.0 | 5.2 |

with increasing content of BMI.$BF_4$. These results are consistent with the values of $R_S$ determined by electrochemical impedance spectroscopy.

The difference between the solution resistances of BMI.$BF_4$ mixtures in EG or GBL media is most likely related to the viscosity of the organic solvent. At 25 °C, the relative permittivity of GBL (42) is similar to that of EG (39) [1, 48]. Therefore, both solvents are able to dissolve true electrolytes, which increases the real number of charge carriers. At 25 °C, the viscosity of GBL is 1.7 cP [1] and of EG is 16.1 cP [49]. A decreased viscosity of the medium causes an increased mobility of charge carriers (i.e., $BMI^+$ and $BF_4^-$), which leads to low-solution resistance values [47].

In a pure BMI.$BF_4$, the high viscosity and ion aggregation lead to low conductivity and high-solution resistance values [46]. Initially, the solution resistance decreases with the addition of EG to the medium. This behavior corresponds to an increase in the number of charge carriers due to the decrease of Coulomb interactions between cations and anions of the ionic liquid [47]. In a medium with low BMI.$BF_4$ concentration, the enhancement in the solution resistance can be explained by a low concentration of ionic species ($BMI^+$ and $BF_4^-$), despite of a high degree of dissociation and high EG amount. In BMI.$BF_4$/GBL mixtures, the decrease of the solution resistance values with the addition of GBL is mainly attributed to the lower viscosity of the solvent compared to EG [47].

The capacitance values for Ni immersed in the mixtures BMI.$BF_4$/EG and in BMI.$BF_4$/GBL are shown in Fig. 6. In both electrolytic systems, the capacitance decreases as the ionic liquid concentration increases.

According to the Stern model [50], the capacitance of the double layer constructed between an electric interface and an electrolytic solution is calculated by the following equations:

$$\frac{1}{C_d} = \frac{1}{C_H} + \frac{1}{C_{GC}} \tag{1}$$

$$\frac{1}{C_d} = \frac{x_H}{\varepsilon_R \varepsilon_0} + \frac{1}{(2\varepsilon_R \varepsilon_0 z^2 e^2 n_i^0 / K_B T)^{1/2} cosh(ze\phi_{\Delta,0}/2K_B T)} \tag{2}$$

Equation 1 indicates that the total capacitance of the double layer ($C_d$) has two contributing sources: the compact, or

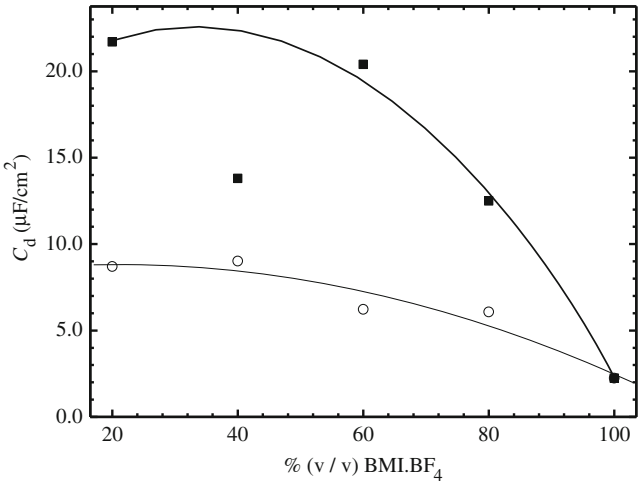


**Fig. 6** A plot of the capacitance ($C_d$) for the Ni electrode as a function of the volumetric percentage of BMI.$BF_4$ in EG (*filled square*) or GBL (*empty circle*) and BMI.$BF_4$ mixtures

Helmholtz, layer ($C_H$) near the electrode surface and the diffuse, or Gouy–Chapmann, layer ($C_{GC}$) inside the solution, which are arranged in series. Equation 2 shows that the first contribution is independent of the potential and that the second is a function of the applied potential. In this equation, $\varepsilon_R$ is the relative permittivity of the double layer, $\varepsilon_0$ is the vacuum permittivity, $x_H$ is the compact layer thickness, $z$ is magnitude of the charge on the ions, $e$ is the charge on the electron, $n_i^0$ is the number concentration of each ion on the bulk, $\phi_{\Delta,0}$ is the potential drop across the diffuse layer, $K_B$ is the Boltzmann constant, and $T$ is the absolute temperature. When the applied potential value is near the potential of zero charge (PZC), $C_H$ is much higher than $C_{GC}$ and $C_d$ is approximately equal to $C_{GC}$. On the other hand, at potentials far from the PZC, $C_{GC}$ is higher than $C_H$ and $C_d$ is equal to $C_H$. Moreover, as the electrolyte concentration increases, the diffuse layer contribution is negligible for the $C_d$ computation. Table 1 shows the molar concentration of BMI.$BF_4$/EG and BMI.$BF_4$/GBL mixtures as a function of volumetric percentage. The values of molar concentration are high, presuming that the most important contribution for the total capacitance is the compact layer capacitance, which is independent of the applied potential.

The Ni electrode/(BMI.$BF_4$+EG) electrolyte interface results in capacitance values greater than the Ni electrode/(BMI.$BF_4$+GBL) electrolyte interface. The capacitance was evaluated at the OCP, while the application of the potential pulse was 10 mV. Previous studies presented that one of the main differences between the electropolishing mechanism in the ionic liquid and the aqueous solution is the rate at which the oxide is removed from the electrode surface [45]. The authors showed that the removal of oxide is a relatively slow process, suggesting that oxide dissolution is the indeed key in the polishing mechanism. This could explain why dissolution appears to occur at small potential pulse in EG medium, which can be sufficient to start a polishing process of the metallic surface by dissolving previous films formed during the preparation of the Ni electrode [44, 45]. However, in the GBL medium, the previous films remain. The double-layer capacitance values formed between an oxide/free metal and an adjacent viscous solution containing metal ions are higher than the capacitance values between a metal and a solution separated by a thin oxide film. The electrolytic capacitors containing dielectric material (metallic oxides) have a capacitance of approximately 0.1 μF/cm² [2]; however, the value for the Ni electrode/(BMI.$BF_4$+EG) electrolyte interface is 22 μF/cm² (i.e., 220 times greater) for 20 and 60 % BMI.$BF_4$. Likewise, the Ni electrode/(BMI.$BF_4$+GBL) systems present capacitance values of nearly 10 μF/cm² (i.e., 100 times greater) for 20 and 40 % BMI.$BF_4$. Hence, smaller values of specific capacitance for the Ni electrode/(BMI.$BF_4$+GBL) electrolyte interface are due to the presence of a thin oxide film formed on the Ni surface during the polishing, rinsing, and drying of the electrode, which act as a dielectric. The variation of capacitance with the volumetric percentage BMI.$BF_4$ (Fig. 6) can be related to the geometric electrode area and also with the presence of ions and dipoles adsorbed.

## Conclusions

The cyclic voltammetry results show that Ni in a BMI.$BF_4$ medium or mixed with EG or GBL (organic solvents), results in a potential range without electrochemical activity. The high capacitance values of the Ni/electrolyte interface observed in these systems should enable the system to be used in electrochemical double-layer capacitors. The best performance is observed for BMI.$BF_4$/EG with 40–20 % (*v*/*v*) or BMI.$BF_4$/GBL with lower than 60 % (*v*/*v*).

**Acknowledgments** Conselho Nacional de Pesquisa (CNPq) and Centro de Microscopia Eletrônica (CME-UFRGS) are acknowledged for their contributions.

## References

1. Ue M (2000) Curr Top Electrochem 7:49–74
2. Juttner K, Lorenz WJ, Paatsch W (1989) Corros Sci 29:279–288
3. Song Y, Zhu X, Wang X, Wang M (2006) J Power Sources 157:610–615
4. Yuyama K, Masuda G, Yoshida H, Sato T (2006) J Power Sources 162:1401–1408
5. Lewandowski A, Galinski M (2006) In: Barsukov IV, Johnson CS, Doninger JE, Barsukov VZ (eds) New carbon based materials for electrochemical energy storage systems: batteries, supercapacitors and fuel cells, 1st edn. Springer, New York, USA
6. Balbucci A, Bardi U, Caporati S, Mastragostino M (2004) Electrochem Commun 6:566–570

7. Ania CO, Pernak J, Stefaniak F, Raymundo-Piñero E, Béguin F (2006) Carbon 44:3113–3148
8. Arbizzani C, Beninati S, Lazzari M, Soavi F, Mastragostino M (2007) J Power Sources 174:648–652
9. Lewandowski A, Swiderska A (2006) Appl Phys A 82:579–584
10. Hsieh C, Chou Y, Chen W (2008) J Solid State Electrochem 12:663–669
11. Frackowiak E (2006) J Braz Soc 17:1074–1082
12. Kuo C, Mare AA (1996) J Electrochem Soc 143:124–130
13. Yuan CZ, Gao B, So LH, Zhang XG (2008) Solid State Ion 178:1859–1866
14. Zhao DD, Bao SJ, Zhao WJ, Hu HL (2007) Electrochem Commun 9:869–874
15. Cui L, Li J, Zhang XG (2009) J Appl Electrochem 39:1871–1876
16. Hummel RE, Smith RJ, Verink ED Jr (1987) Corros Sci 27:803–813
17. Martini EMA, Amaral ST, Muller IL (2004) Corros Sci 46:2097–2115
18. Moore KL, Sykes JM, Grant PS (2008) Corros Sci 50:3233–3240
19. Trombetta F, de Souza MO, de Souza RF, Martini EMA (2009) J Appl Electrochem 39:2315–2321
20. Galinski M, Lewandowski A, Stephniak I (2006) Electrochim Acta 51:5567–5580
21. Greaves TL, Drummond CJ (2008) Chem Rev 108:206–237
22. Tsuda T, Hussey CL (2007) Electrochem Soc Interface 16:42–49
23. Yang W, Cang H, Tang Y, Wang J, Shi Y (2008) J Appl Electrochem 38:537–542
24. de Souza RF, Padilha JC, Gonçalves RS, Dupont J (2003) Electrochem Commun 5:728–731
25. Sato T, Marukane S, Narutomi T, Akao T (2007) J Power Sources 164:390–396
26. Song Y, Liu L, Zhu X, Wang X, Jia H, Yang X (2008) Solid State Ionics 179:516–521
27. Baldelli S (2008) Acc Chem Res 41:421–431
28. Sirieix-Plénet J, Gaillon L, Letellier P (2004) Talanta 63:979–986
29. Inoue T, Ebina H, Dong B, Zheng LQ (2007) J Colloid Interface Sci 314:236–241
30. Baltazar QQ, Chandawalla J, Sawyer K, Anderson JL (2007) Colloid Surface-A 302:150–156
31. Bandrés I, Montaño DF, Gascón I, Cea P, Lafuente C (2010) Electrochim Acta 55:2252–2257
32. Padilha JC, Basso J, Trindade LG, de Souza MO, de Souza RF (2010) J Power Sources 195:6483–6485
33. Blanchard LA, Hancu D, Beckman EJ, Brennecke JF (1999) Nature 399:28–29
34. Tran CD, Mejac I, Rebek L Jr, Hooley RJ (2009) J Anal Chem 81:1244–1254
35. Perissi I, Bardi U, Caporali S, Lavacchi A (2006) Corros Sci 48:2349–2362
36. Trombetta F, Borges CB, Panno NF, de Souza RF, de Souza MO, Martini EMA (2011) Corros Sci 53:51–58
37. Suarez PAZ, Dellius JEL, Einloft S, de Souza RF, Dupont J (1996) Polyhedron 15:1217–1219
38. Dupont J, Consorti CS, Suarez PAZ, de Souza RF (2002) Org Synth 79:236–239
39. Barrose-Antle LE, Bond AM, Compton RG, O'Mahony AM, Rogers EI, Silvester DS (2010) Chem Asian J 5:202–230
40. Rogers EI, Silvester DS, Poole DL, Aldous L, Hardacre C, Compton RG (2008) J Phys Chem C 112:2729–2735
41. O'Mahony AM, Silvester DS, Aldous L, Hardacre C, Compton RG (2008) J Chem Eng Data 53:2884–2891
42. Fushimi K, Kondo H, Konno H (2009) Electrochim Acta 55:258–264
43. Sjostrom T, Su B (2011) Mater Lett 65:3489–3492
44. Lee BG, Hong SY, Yoo JE, Choi J (2011) Appl Surf Sci 257:7190–7194
45. Abbott AP, Capper G, McKenzie KJ, Ryder KS (2006) Electrochim Acta 51:4420–4425
46. Dupont J (2004) J Braz Chem Soc 15:341–350
47. Zhu A, Wang J, Han L, Fan M (2009) Chem Eng J 147:27–35
48. Awwad AM, Al-Dujaili AH, Salman HE (2002) J Chem Eng Data 47:421–424
49. Tsierkezos NG, Molinou IE (1998) J Chem Eng Data 43:989–993
50. Bard AJ, Faulkner LR (2001) Electrochemical methods: fundamentals and applications. Wiley, New York, pp 534–579